

## Article

# Investigation of Rheological Test Methods for the Suitability of Mortars for Manufacturing of Textile-Reinforced Concrete Using a Laboratory Mortar Extruder (LabMorTex)

Matthias Kalthoff , Michael Raupach  and Thomas Matschei

Institute of Building Materials Research (IBAC), RWTH Aachen University, Schinkelstraße 3, 52062 Aachen, Germany

\* Correspondence: matthias.kalthoff@rwth-aachen.de; Tel.: +49-241-80-95143

**Abstract:** One of the promising technologies to produce carbon textile-reinforced concrete structures is extrusion. For defect-free extrusion, high requirements are placed on the fresh concrete, since it must be transportable through the augers in the extruder and must not change the desired geometric shape after leaving the mouthpiece. For the rheologic description of suitable concretes or mortars for the extrusion process, there is currently a lack of test methods to characterise the fresh concrete before extrusion. At present, new mixtures are first tested in elaborate trials on laboratory extruders before they can be transferred to production scale. The development of compounds is strongly dependent on the know-how and experience of the users. Within the scope of this paper, different methods were investigated and systematic suitability tests for a successful extrusion have been carried out. The results show that the fresh mortar can only be roughly described by the measured data during the mixing process, such as the temperature or the torque. The use of a capillary rheometer only allows a basic characterisation of the fresh mortar. A clear differentiation of the fresh mortar can be made with the help of sphere penetration tests. These allow the mortar to be classified as unsuitable for the extrusion process or as extrudable before the extrusion process, and the suitability of new mixtures can be assessed in advance. The newly developed method offers the possibility of greatly accelerating the implementation of new formulations for the extrusion process, regardless of the experience of the subsequent users, and reducing the need for complex experiments using laboratory extruders.

**Keywords:** extrusion; rheology; test method; textile-reinforced mortar



**Citation:** Kalthoff, M.; Raupach, M.; Matschei, T. Investigation of Rheological Test Methods for the Suitability of Mortars for Manufacturing of Textile-Reinforced Concrete Using a Laboratory Mortar Extruder (LabMorTex). *Constr. Mater.* **2022**, *2*, 217–233. <https://doi.org/10.3390/constrmater2040015>

Received: 16 August 2022

Accepted: 26 September 2022

Published: 29 September 2022

**Publisher's Note:** MDPI stays neutral with regard to jurisdictional claims in published maps and institutional affiliations.



**Copyright:** © 2022 by the authors. Licensee MDPI, Basel, Switzerland. This article is an open access article distributed under the terms and conditions of the Creative Commons Attribution (CC BY) license (<https://creativecommons.org/licenses/by/4.0/>).

## 1. Introduction

Over the last decade, many research efforts have concentrated on the digitalisation of the building industry. One focus is the development of novel additive manufacturing processes, with 3D concrete printing as the main research subject [1–3]. In addition to 3D concrete printing, concrete components can also be produced using the classic extrusion process as it is described in the literature [4–7]. These two processes cannot always be clearly separated from each other. In the context of this paper, a distinction is therefore made between classical extrusion (moulding) and robot-assisted processes such as 3D concrete printing. We define extrusion as a production process in which viscous materials are continuously pressed through a shaping mouthpiece, giving the extrudate its final shape.

To extrude cement-bound concrete without defects, many general conditions must be met, and the rheological behaviour of the material must be adapted to the process technology. The adjustment and control of the consistency of the concrete for the extrusion process is rheologically complex [8]. Imperfections or unusable extrusion products can occur even with the smallest deviations in the setting behaviour or the consistency of the fresh concrete [4,9,10]. In addition, the use of so-called extrusion aids such as methyl cellulose is of central importance for flawless classical extrusion [11]. The methyl cellulose, in combination with water, forms a gel-like mass that includes the solid particles and

thereby traps air, resulting in a smooth and plastic consistency of the fresh concrete. After leaving the mouthpiece, the gel structure ensures that the geometric shape is maintained and the extruded specimen has developed sufficient green strength [12,13].

The concrete mixes for the extrusion process [4–6,8] as well as for 3D concrete printing [10,14–19] have to be soft enough to be transported and yet stiff enough to retain the desired shape when leaving the mouthpiece [8,11,20]. In addition to unreinforced mixes, fibre-reinforced mixes are usually used to additionally stabilise the fresh concrete and to counteract possible shrinkage cracks, as perfect finishing is usually difficult to achieve [12,21–23]. Different types of fibres, e.g., from recycled materials [24], can be used even in geopolymer concrete mixes [25].

There is no test method to precisely determine the flow behaviour of rigid masses during extrusion [26]. The flow behaviour of the extruded masses depends to a large extent on the time of measurement, the mixer, moisture content, particle size distribution, mineralogical composition, additives such as methyl cellulose and the vacuum applied in the extruder.

In ceramics, the term “plasticity” is often used to describe the rheological behaviour. However, the terms “extrudability”, “ductility”, “consistency” and “workability” are also used as synonyms [8,27–30]. In order to enable an adequate description of stiff masses, there are several test methods which are used depending on the type of material. In this paper, we concentrate only on the most relevant methods. In classical extrusion, e.g., in ceramics, hand penetrometers are often used for an initial estimate during production [28]. A stick is pressed into the extrudate and the penetration resistance is measured. The non-standardised Pfefferkorn method [31] is also frequently used to determine the rheological parameters, such as the yield stress. Furthermore, kneading tests and compression tests are used to investigate the consistency of the clays [28].

A capillary rheometer is often used in both the ceramics and plastics industries, as well as in concrete construction. This usually consists of a cylinder with a taper at the bottom. This taper can be designed as an exchangeable nozzle in different geometric shapes. For the test, a defined quantity of the material to be tested is filled into the cylinder and moved downwards with the help of a piston that is clamped in a testing machine. The test speed is usually applied at a constant rate and the material is pressed through the nozzle. The measured values obtained in this way can be used to determine the flow properties such as shear stress, shear rate and wall shear stress. The design of the capillary rheometer can vary greatly between the individual fields of application [8,9,32–36]. Often, new extrusion compounds are also tested on small extruders and then scaled up for plant-scale application.

Penetration tests are often used in the field of geotechnics or 3D concrete printing to characterise soils or cementitious materials [37–39]. The Vicat test, in which the penetration resistance of a needle is measured during the hardening of the concrete, is a well-known penetration test in the field of mortar and cement paste. The method is not suitable for concrete because of the large aggregate grains involved. Either the penetration resistance under a defined speed or the penetration depth at a constant load is measured. The resistance of the material is described with the help of the determined results [38–40]. The yield stress of the material can be determined by a very slow speed (approx. 1  $\mu\text{m/s}$ ) [38,39,41]. The yield stress provides information about the plasticity and can be used as an indicator for extrudability [7,42].

In addition to the methods already described, the slump test is often used in 3D concrete printing to describe the consistency of relatively soft fresh concretes [43,44]. Shear tests, for example, in [45] using a rheometer, or the squeeze-flow test [46] are additionally carried out [20] to assess the rheological properties of the concrete used for 3D printing applications. The methods are always adapted depending on the reactivity of the concrete mix or the change in consistency over time.

There are two different approaches to 3D concrete printing. The first approach is that the mixture is initially set comparatively soft and accelerators are only added shortly before the concrete leaves the nozzle [47,48]. This means that the consistency of the concrete

changes considerably in a short time, which makes a rheological description difficult. The second approach is to set the consistency so stiff that the layer build-up only works without accelerators due to the high green strength. This approach leads to an increased closure and a high wall friction in the pipes during printing [49,50].

In the classic extrusion of cement-based materials, even stiffer compounds are usually used [5,7]. This is possible because the concrete leaves the mouthpiece immediately after being conveyed through the screw in the extruder, and there is no transport through long pipes. Additionally, there is usually no layer build-up, which means that no connection between two concrete layers has to be ensured. The component is therefore only defined by the geometry of the mouthpiece [5,6].

The rheological description of highly viscous concretes with a stiff consistency for the extrusion process is complex in terms of testing. Hence, the usual fresh concrete tests such as the flow test or slump tests cannot be applied. At present, the suitability of concretes for the extrusion process is usually tested iteratively on laboratory extruders, despite the large number of rheological test methods available. The test methods described above are used, but these methods are currently highly inaccurate because they do not detect the smallest differences in the changes in the raw materials and the consistency, which means that the development of new mixes is time-consuming and mostly depends on the experience of the employees.

In this paper, different methods are tested to rheologically characterise mortars for a laboratory mortar extruder (LabMorTex, manufactured by Händle GmbH, Mühlacker Germany; see [5,6,51]) during the mortar mixing process and immediately after the end of the mixing. The aim is to determine the suitability of the fresh mortar before the extrusion with textiles. At present, there is a lack of knowledge as to how the suitability of the compound for defect-free extrusion can be concluded from the rheological parameters.

**2. Materials**

Several methods have been investigated at the Institute for Building Materials Research at RWTH Aachen University which enable us to characterise the mortar extrudability immediately after mixing and before the actual extrusion process. The aim of the investigations is to develop a method which describes the fresh mortar consistency sufficiently to distinguish between successful extrudable and non-extrudable textile-reinforced mortar components.

Therefore, 13 mortars of different consistencies and compositions were rheologically characterised within the scope of this work. The mixture compositions can be found in Table 1. Mixtures 3, 11, 12 and 13 are not suitable for the extrusion process used in this work. The classification into extrudable and non-extrudable components is discussed in more detail in Section 3.2 of this paper.

**Table 1.** Mix design of the investigated mortars.

Components	Unit	1	2	3	4	5	6	7	8	9	10	11	12	13
CEM I 42.5 R				400			550		700	700	700	700	700	700
CEM III/A 42.5 N				-			-	700	-	-	-	-	-	-
Silica fume powder				40			55	70	70	70	70	70	70	70
Fly ash				120			165	210	210	210	210	210	210	210
Water	kg/m <sup>3</sup>			278			278	278	278	278	278	278	278	278
Sand 0.1–0.5 mm		658	658	670	670	633	670	675	679	670	675	850	850	585
Quartz powder 0–0.250 mm		271	273	278	278	263	278	280	282	278	280	353	353	243
Quartz powder 0–0.063 mm				404			208	-	-	-	-	-	-	-
PVA microfibres		6.5	6.5	-	-	-	-	-	-	6.5	3.3	-	-	-
Basalt microfibres		-	-	6.5	6.5	6.5	6.5	3.3	-	-	-	6.5	6.5	6.5
Methyl cellulose		7.0	7.0	7.0	7.0	7.0	7.0	7.0	7.0	7.0	7.0	7.0	7.0	7.0
Extrudable		Yes	Yes	No	Yes	No	No	No						

The two microfibres were used to increase the stability of the fresh concrete. In addition, the fibres should prevent the formation of shrinkage cracks on the surface or cause potential cracks to be distributed, thus creating cracks with low crack widths. It could already be shown in [5,6] that the microfibres in the contents investigated here had no significant influence on the compressive and flexural strength. The main material properties of the used microfibres can be found in Table 2.

**Table 2.** Material properties of the used microfibres (manufacturer data).

Fibre	Tensile Strength	Youngs Modulus	Density	Diameter	Length
Unit	MPa	GPa	g/cm <sup>3</sup>	µm	mm
PVA fibre	1600	39	1.30	26	6
Basalt fibre	860	68	2.65	13–16	6

**3. Methods**

*3.1. Mortar Production*

As no standard fresh concrete procedure could be carried out due to the extremely high stiffness, the first step was to use the mixer data for the rheological classification of the mixes. Analogous to the studies from [5], an Eirich R05T intensive mixer with a maximum capacity of 40 L was used to produce the mortars for the extrusion process. With the mixer, the drum as well as the mixing paddle can be controlled separately. Furthermore, the motor data, the temperature in the mixer and the resistance torque can be recorded during mixing. For each batch, 18 L of fresh mortar were produced. First, the dry components were homogenised at 500 revolutions per minute for a duration of a minute. Then, the water was added within 15 s at 66 revolutions per minute. The mortar was then mixed for a further 130 s at 800 rpm. Finally, the revolutions per minute were reduced at intervals of 100 revolutions per minute every 15 s to investigate the rheological behaviour of the compounds at different loads. During the mixing process, the mixing data were also recorded. The diagram in Figure 1 shows the exemplary mixing data for mixture 1.

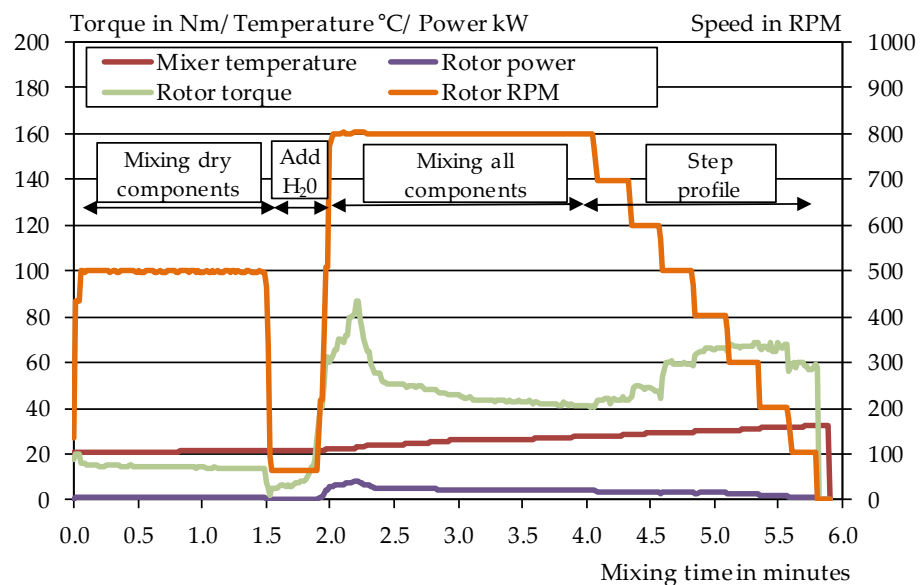


**Figure 1.** Mixing process of the extruded mortar using mix 1.

On the primary Y-axis, the measured rotor torque, the temperature in the mixer and the motor power are shown. For a better overview, the present RPM of the rotor over the mixing time is shown on the secondary axis. The recorded data from each mix was analysed and should give an initial indication of the consistency of the extremely stiff concrete. The mixing regime was kept the same for all of the mixtures.

### 3.2. Mortar Extrusion Process

A Händle laboratory extruder was used for the extrusion of the textile-reinforced mortar. The extrusion process of the laboratory mortar textile extruder (LabMorTex) has already been presented in detail in [5,6]. Therefore, the procedure is only briefly summarised here. This consists of a pre-press and an auger. Various mouthpieces in different geometries can be attached to the end of the auger. The diameter of the main auger is around 70 mm. In the transition area between the pre-press and the main auger, it is also possible to generate a vacuum which de-airs and compresses the extrudate. Along the auger, it is possible to regulate the temperature of the mortar through the double-walled housing. Figure 2a shows a photo of the extruder and Figure 2b shows a technical drawing. After the mortar has left the mouthpiece, it is transported on a conveyor belt.

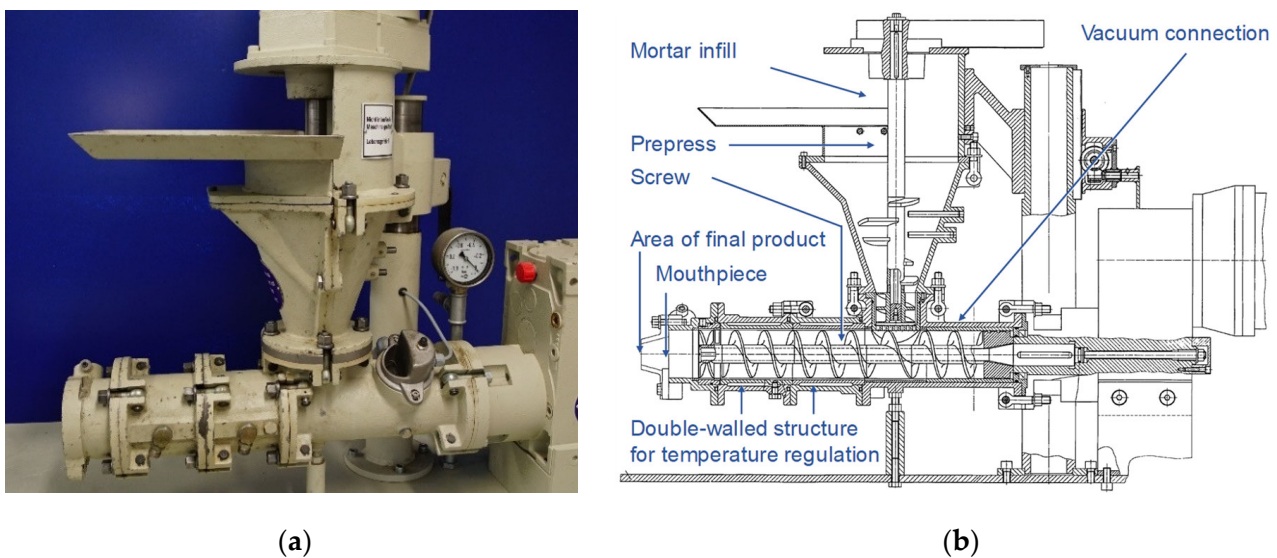


**Figure 2.** (a) Laboratory mortar extruder [5] and (b) schematic drawing of the laboratory mortar extruder [5].

Immediately at the end of the auger, the pressure in bar and the temperature in °C are measured during extrusion. In addition, the speed in rpm, the motor current in amperes of the auger and the pre-press as well as the negative pressure generated by the vacuum pump are measured. By means of a measuring impeller, it is also possible to monitor the attached conveyor belt speed.

In order to evaluate the different compounds rheologically, all of the mixtures in Table 1 were tested with the described extrusion process, thereby a distinction can be made between three consistency classes. The mix is either too soft, extrudable or too stiff. Whether a mortar is suitable for the extrusion process depends on a number of factors such as: the type of extruder, the age of the fresh mortar, the type of mouthpiece and the extrusion speed. In the context of this work, a mortar is therefore considered extrudable if it retains the desired geometric shape after leaving the mouthpiece and no defects such as cracks are visible on the mortar surface.

Different mouthpiece geometries are available for the extrusion process. In the context of this work, the extrudability was determined on a prismatic cross section of the dimension 10 mm × 60 mm. The prismatic shape has four corners and a low height, which is much more demanding for a successful extrusion process compared to a round mouthpiece, as the mortar has to be formed more extensively in the mouthpiece. Furthermore, the prismatic shape is also used for the production of the textile-reinforced mortar from the preliminary work from [5]. A picture of the applied mouthpiece is shown in Figure 3a.

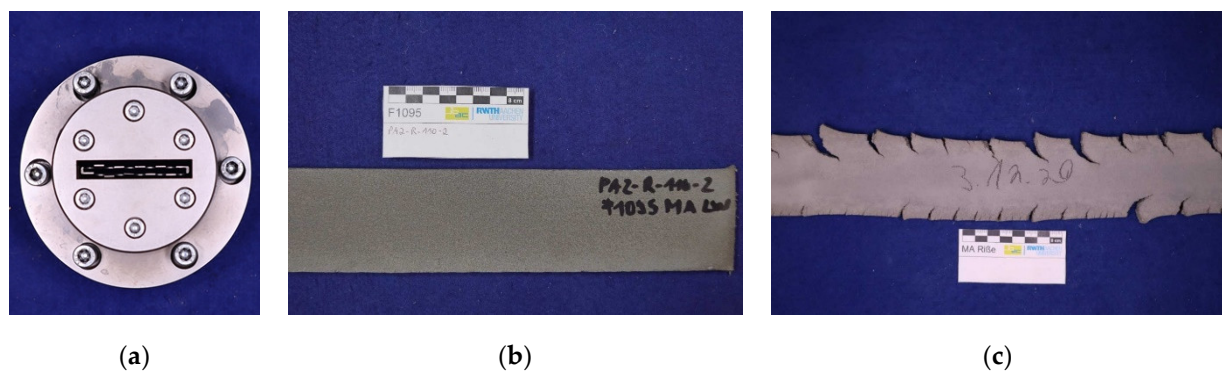


**Figure 3.** (a) Mouthpiece for the extrusion of textile mortar, cross section  $60 \times 10$  mm, (b) example of a suitable mixture for the extrusion process, (c) example of an unsuitable mixture for the extrusion process.

An example of a successful extrusion can be found in Figure 3b where no defects on the surface or string widening could be detected. In the case of unsuccessful extrusion in Figure 3c, the mortar string ruptured and it was not possible to produce uniform test specimens. Within the scope of this work, nine mortars could be successfully extruded, as shown in Figure 3b, and four mortar mixes failed, as shown in Figure 3c. An overview of the extrudability of the investigated compounds can be found in Table 1.

### 3.3. Material Characterisation

#### 3.3.1. Penetration Tests

To characterise the fresh mortar rheologically, penetration tests with steel spheres were carried out on all of the mixtures. Immediately after production, 5 kg of fresh mortar was filled into a plastic cylinder with a height of 15 cm and a diameter of 20 cm. To achieve a representative mortar surface, the fresh mortar was then compacted in a hydraulic press by pressing on a 20 mm thick plastic disc up to a pressure of 50 bar, which created a flat surface while reducing the cavities in the fresh mortar.

The cylinder was then placed in the universal testing machine 5566 from ZwickRoell GmbH & Co. KG (Ulm, Germany). The actual penetration test was carried out with three stainless steel spheres, which only differed in diameter (10 mm, 15 mm and 20 mm). The steel spheres are mounted on a punch which has a smaller diameter than the actual spheres, so that the mortar is only pressed in by the steel sphere and so the coat friction of the punch during penetration could be excluded. A schematic sketch of the test set-up is shown in Figure 4a and a photo during the test in Figure 4b. The spheres were inserted into the fresh mortar at a test speed of 1 mm/s to a depth of 30 mm.

The testing machine records the penetration force and testing time, while the crosshead moves through the sample. The penetration test was repeated at seven points with the three different sphere diameters for all mortar compounds. The arrangement of the seven penetration points is shown in Figure 5a,b. The first test was always done in the middle of the cylinder cross section. The six other penetration points were positioned clockwise around the centre of the cylinder. The distance to the edge of the cylinder was approximately 3 cm. All of the test points were selected by eye. The positions were chosen at points where the fresh mortar surface was homogeneous and without defects. The test was carried out 20 min, 40 min and 60 min after the end of the mixing in order to assess the change in fresh concrete consistency over the period in which the test specimens are produced, according to experience. The first seven trials were always carried out with the largest 20 mm diameter sphere. These tests were started about 20 min after the start of the mixing. After the cylinder had been cleaned, refilled and compressed, the 15 mm diameter sphere was used. This was done approximately 40 min after the start of the mixing. After renewed filling and compression, seven penetration tests were carried out for the third time. In this case, the smallest sphere with a diameter of 10 mm was used. The tests were started

about 60 min after the start of the mixing. From the end of the mixing until the end of the penetration tests, the fresh mortar was stored in an airtight box.

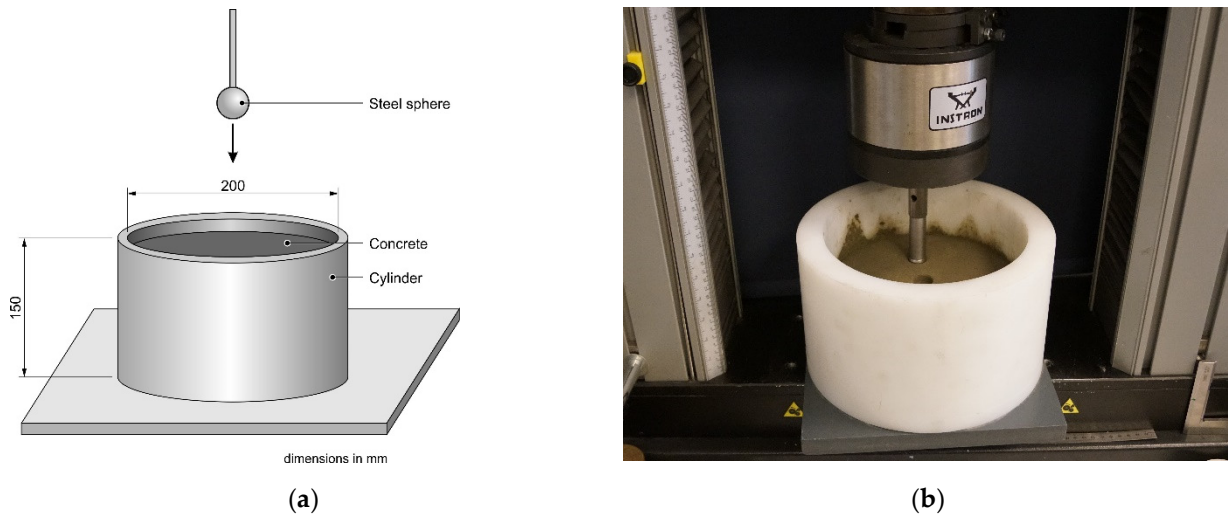


**Figure 4.** Sketch of the experimental set-up of a penetration test (a) and recording of the penetration of the sphere (b).

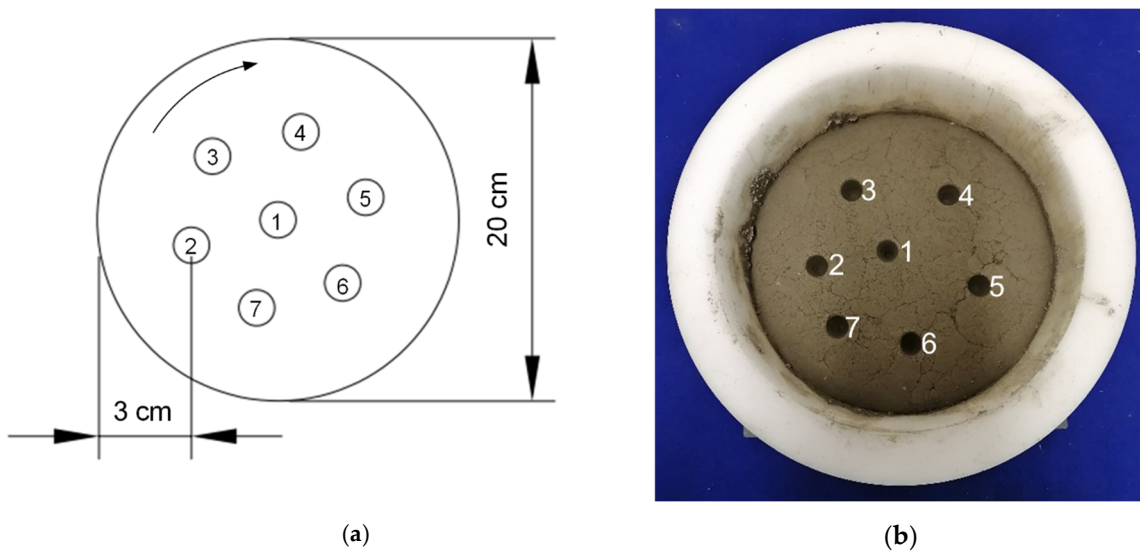


**Figure 5.** Arrangement of the penetration points 1–7 (a) and example of a fresh mortar sample tested with the 15 mm diameter sphere (b).

### 3.3.2. Capillary Rheometer

As a further method, a capillary rheometer was developed and built based on the work described in [8]. The capillary rheometer consists of two cylinders, a connecting and supporting element and a plunger. A connection for a pressure sensor is provided on each of the two cylinders. These are located just in front of and just behind the connecting piece. The construction of the capillary rheometer is shown in Figure 6.

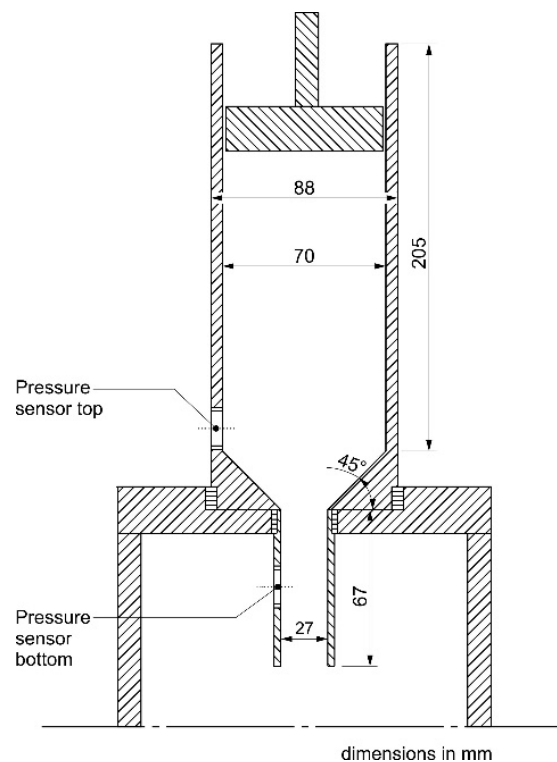


**Figure 6.** Sketch and dimensioning of the capillary rheometer test set-up based on [8].

The upper cylinder has an inner diameter of 70 mm and a height of 205 mm. The inner diameter of the upper cylinder was chosen based on the geometry of the extruder's main screw. The lower cylinder has an inner diameter of 27.6 mm and a height of 67.0 mm. The resulting cylinder opening has a cross-sectional area of around 600 mm<sup>2</sup> and thus corresponds to the cuboid with 10 mm × 60 mm, which is also used to assess the extrudability. The aim of this experimental set-up is to simulate the flow behaviour of the fresh mortar realistically during extrusion with little effort. The two cylinders are screwed together with the conical connecting element so that the cross section decreases from top to bottom. In the connecting piece of the two cylinders there is a truncated cone through which the cross section is tapered at a 45-degree angle in diameters from 7.0 to 27.6 mm.

Both the stamp and a Teflon disc with a thickness of approximately 5 mm, which is located between the fresh mortar and the stamp during the test, have a marginally smaller diameter (approx. 69.5 mm) than the larger cylinder. This allows the stamp to be pressed into the larger cylinder with an almost perfect fit and the air remaining in the test mass between the Teflon disc/stamp and the inside of the cylinder to escape.

A total of 1.2 kg of fresh mortar was filled into the upper cylinder. The mortar was compacted with a wooden pestle during the filling process. The Teflon disc was then placed on the mortar surface. At the beginning of the test, the ram was moved downwards at a speed of 1 mm/s. The time was also measured. In addition to the time, the crosshead travel, the force and the pressures of the two pressure sensors were also measured and recorded. The mortar was thus forced through the taper and exited the capillary rheometer at the bottom of the lower cylinder. This test was carried out once for each of the 13 mixes approximately 20 min after the end of the mixing.

#### 4. Results and Discussion

This chapter presents the test results for the rheological description of plastic mortars for the extrusion process. For this purpose, the evaluation of the mixer process data and the penetration and capillary rheometer experiments are presented first. For a better overview, the non-extruded mixtures are shown below as dotted lines.

4.1. Mixing Energy and Rotor Torque

Figure 7 shows the relative temperature changes in all the tested mixtures from the beginning of the mixing process. During dry mixing, only a slight increase in temperature of approx. 1 Kelvin can be seen. As expected, there is only a significant increase in the measured temperature in the mixer after the addition of water.

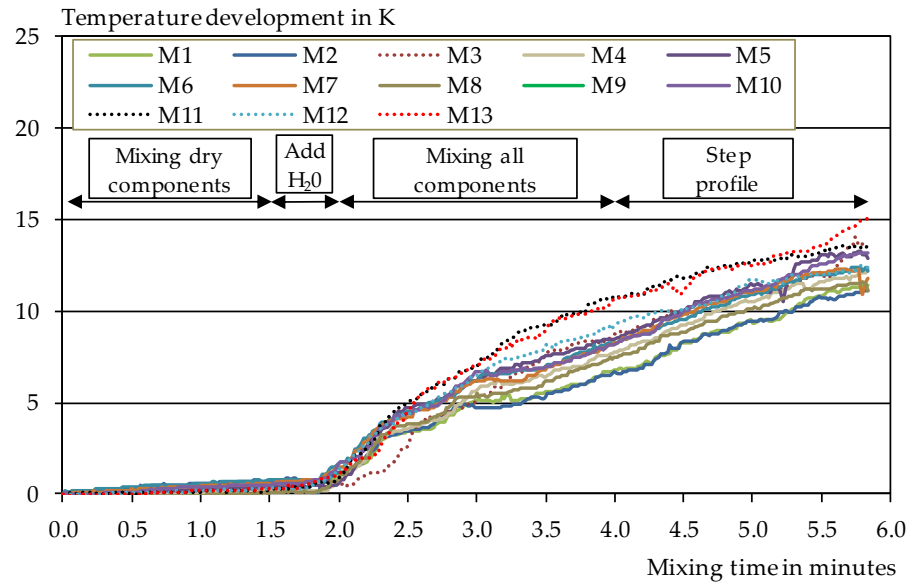
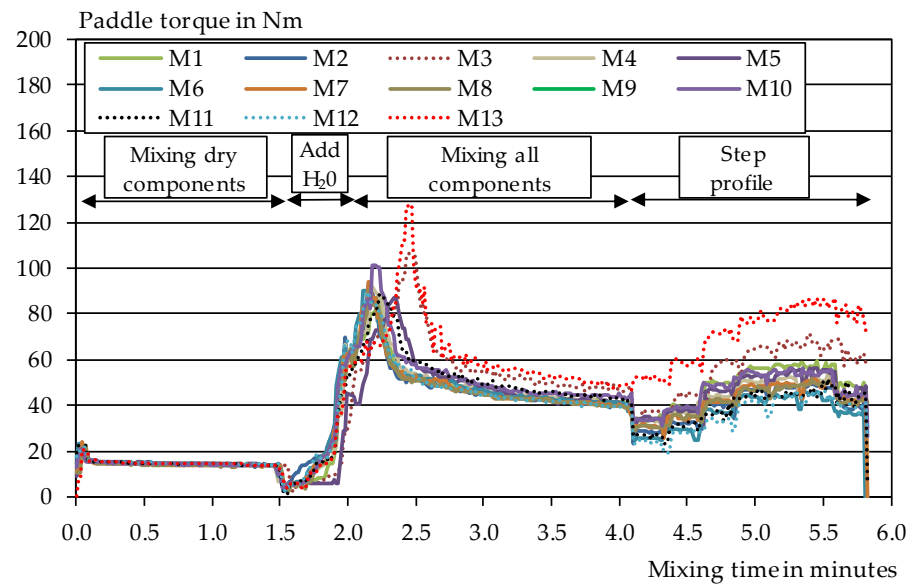


Figure 7. Relative temperature increase from the start of mixing for all mixtures. Non-extractable mixtures are shown in dotted lines.

The temperature in the mixer tends to rise more for the mixtures that are too stiff, and are therefore not extrudable, than for the extrudable mixtures. This is due to the increased stiffness of the fresh mortar which prevents a successful extrusion. The maximum temperature increase was observed in mix M13 and amounted to approximately 15 K. During the extrusion process, the mortar cools down again to a temperature of about 22 °C and does not change significantly during extrusion. This is mainly due to the large contact area of the mortar with the steel in the extruder which is at room temperature. However, the mixes cannot be clearly separated from each other, which means that a prediction for extrudability is not possible from the temperature curves alone.

Figure 8 shows the measured torque during the mixing process for all of the mixtures. During dry mixing, the measured torque is approximately the same for all of the mixtures. The decrease with the beginning of the addition of water is related to the reduction in the speed. Immediately after the addition of water, the torque also increases here. Mixture 3 and mixture 13 show the highest measured torque, which can be attributed to a stiff fresh mortar consistency. At the beginning of the wet mix, the high torque can also be explained by the acceleration of the mixing paddle. With good mixing, the resistance decreases again. However, as before, there is no clear distinction between the extrudable and the non-extrudable mixtures, which means that the measured torque cannot be used as a clear characteristic value for assessing the extrudability.

After 4 min, the speed was reduced successively in the form of a step profile. Here it can be clearly seen that the section modulus increases with a decreasing speed. This rheological thixotropic behaviour is crucial for extrusion and allows the mortar to maintain the desired geometric shape after leaving the mouthpiece.



**Figure 8.** Measured torque from start of mixing for all compounds. Non-extrudable mixtures are shown as dotted lines.

Based on the step profile in the mixing process, approximate flow curves were calculated for the mixtures investigated using a simple Bingham model [52]. The results can be found in Figure 9. It should be mentioned here that this is a great simplification and that the mixer is not a classic rheometer. However, it is not possible to differentiate clearly between the individual mixtures. Mixtures 3 and 13 show the highest yield stress, but mixture 12 and mixture 11 do not differ from the other extrudable mixtures. Thus, only a tendency for the extrudability of the individual compounds can be derived from the mixer data. Extremely stiff and soft consistencies can be identified, but the discriminatory power of all three parameters is not sufficient for a differentiated classification of the compound.

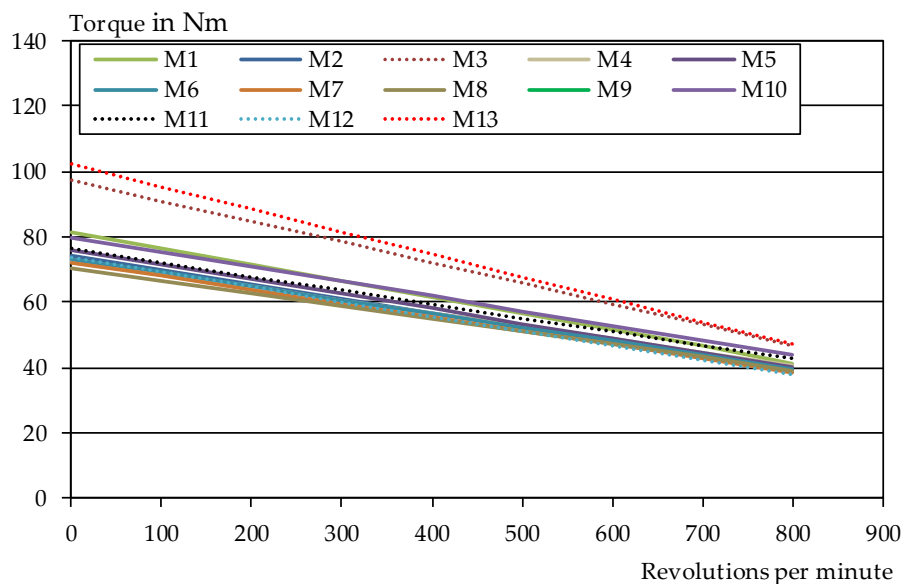


**Figure 9.** Determined flow curves from mixer data for all mixtures. Non-extrudable mixtures are shown as dotted lines.

#### 4.2. Capillary Rheometer

To simulate the rheological behaviour of the fresh mortar in the extruder as realistically as possible, a capillary rheometer was used, which was built according to the dimensions

of the laboratory extruder. The measured pressures are significantly lower than the results from [8] for example, which is due to the different mixtures as well as the high velocities. The conical taper made it possible to avoid dead zones, as described in [9].

The results of the measured pressures immediately before tapering are shown in Figure 10. Again, the stiff, non-extrudable compounds M3 and M11 showed the highest measured pressures during the test. Occasionally, abrupt drops in pressure were recorded during the test. Here it can be assumed that the compaction of the fresh mortar by the ram before the actual test was not sufficient to remove all the large air pockets from the fresh mortar. This led to the mortar only being compacted in the capillary rheometer.

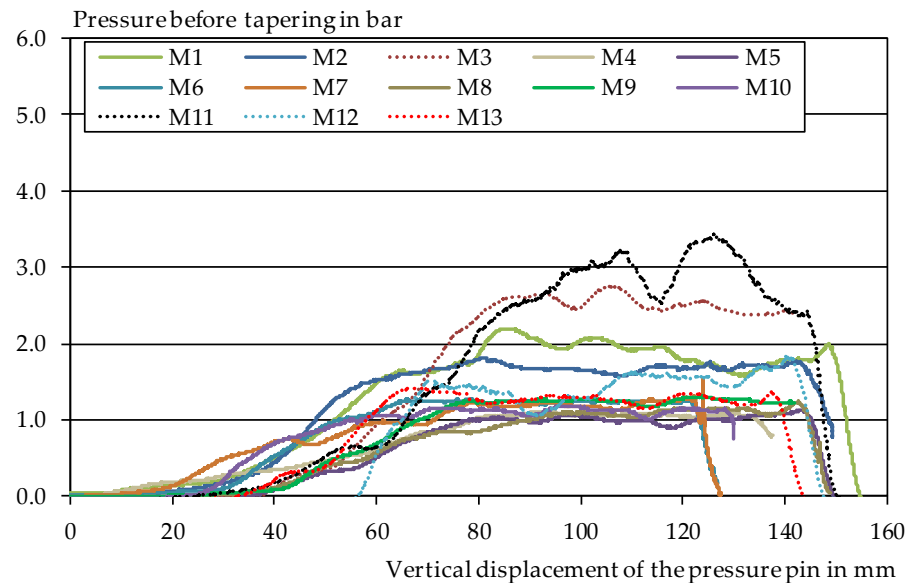


**Figure 10.** Measured pressure during the test immediately before tapering in the capillary rheometer for all mixtures. Non-extrudable mixtures are shown as dotted lines.

However, in this test the mixtures 13 and 12 cannot be distinguished from the extrudable mixtures. The results of the measured pressure immediately after tapering in Figure 11a also do not allow a clear differentiation of the fresh mortar. At this point, only the friction of the fresh mortar is measured, which means that no further rheological parameters can be derived.

Figure 11b shows the standard deviation of the measured pressures during the test for mixture 3 and mixture 9 as examples for a better overview. The scatter of the measured pressures during the tests is not particularly large. The results of the investigations showed that the rheological description of the mortars is generally possible in the same way as in [8,9,32], for example. For a precise differentiation of the fresh mortar, this type of capillary rheometer seems unsuitable to classify the used mortars as too stiff for extrusion or extrudable.

#### 4.3. Penetration Tests

To evaluate the recorded data from the penetration tests, the contact area of the sphere with the mortar during penetration was first determined for all measured values of the penetration depth. From a penetration depth exceeding half the diameter of the sphere, the contact area was determined by half the surface area of the sphere.

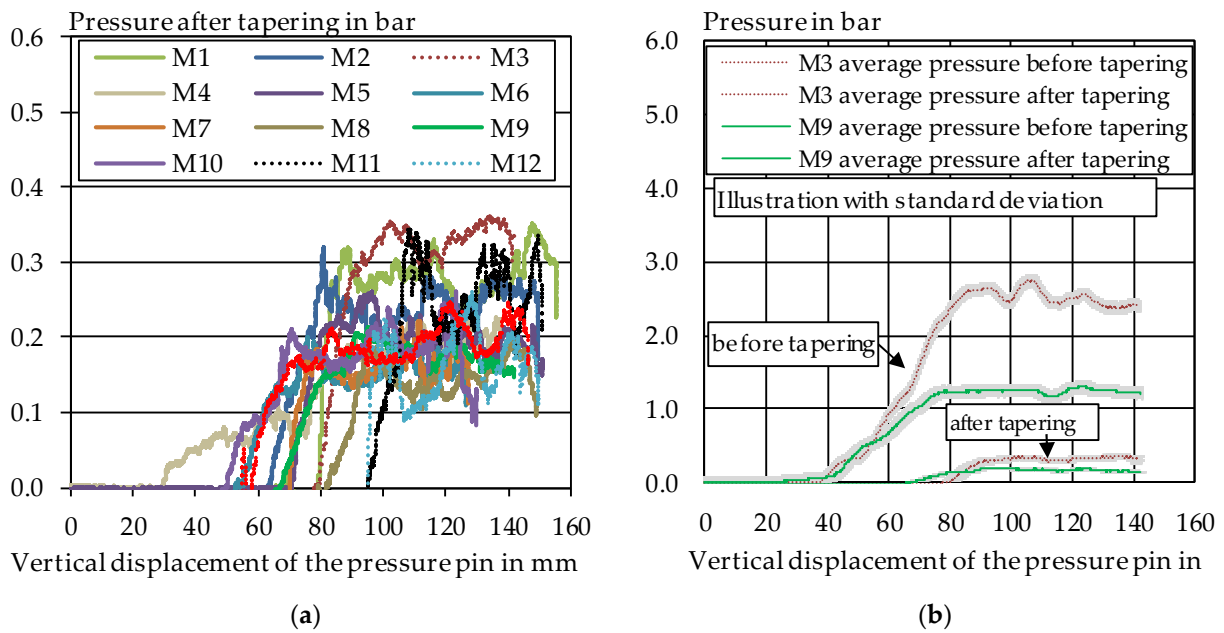


**Figure 11.** (a) Measured pressure during the test immediately after tapering in the capillary rheometer for all compounds. Non-extrudable mixtures are shown as dotted lines, (b) measured pressure during the test before and immediately after tapering including standard deviation for M4.

By dividing the recorded forces by the contact area, the resistance stress in MPa was determined, which describes the penetration resistance of the sphere during the test as a function of the respective penetration depth. A characteristic point can be seen for all compounds as soon as the penetration depth corresponds to half the sphere diameter. An example of this is shown in Figure 12. Since this point could be clearly identified for all of the mixtures, it was used for the evaluation of the penetration tests. In addition, this ensures that the mortar collapses above the sphere and thus influences the measurement of the penetration resistance.

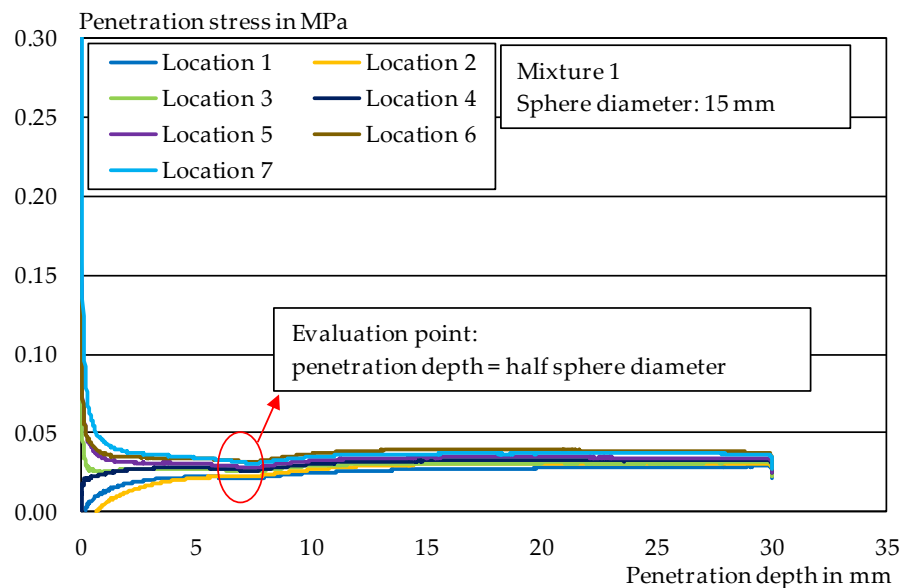


**Figure 12.** Results of the penetration tests carried out on mixture M1 with sphere diameter 15 mm.

Based on the evaluation from Figure 12, the corresponding indentation stresses were determined for all seven indentation points of a series. Figure 13 shows an example of this for mixture 1. It can also be seen that the indentation stress increases over time.

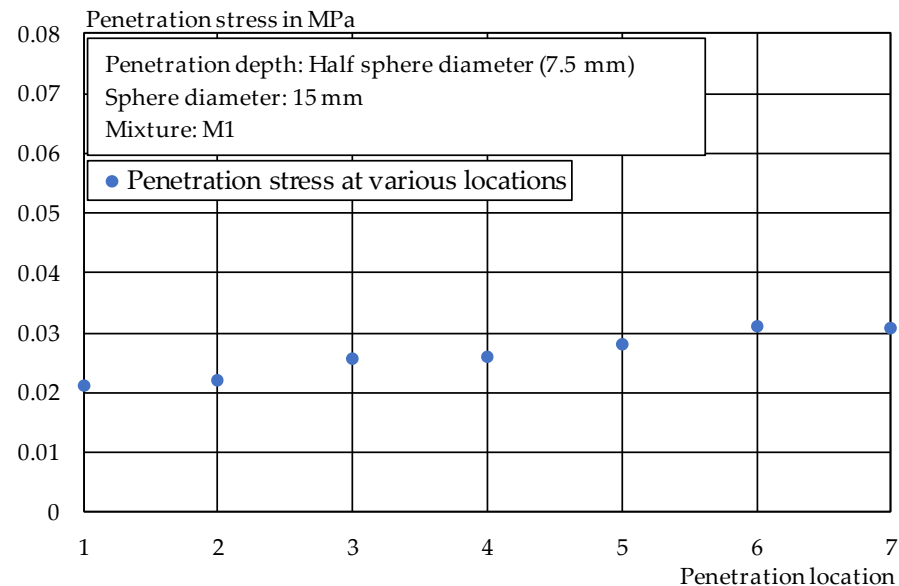


**Figure 13.** Resistance stresses at the time when the penetration depth corresponds to the sphere radius of 7.5 mm (sphere diameter 15 mm), mixture M1.

This can be explained by an increasing hydration and the dehydration of the fresh mortar on the mortar surface. To obtain a representative statement on the penetration behaviour of the spheres, the individual penetration stresses were averaged for each measurement. Figure 14a shows the results of the indentation tests as a function of the selected sphere diameter. Regardless of the selected diameter, all compounds which are apparently too stiff and therefore cannot be extruded can now be distinguished from the compounds that can be extruded. Compared to the other measuring methods, the penetration test enables a clear characterisation of the fresh mortar, with which it can be classified as too stiff for extrusion or extrudable.

As expected, the results suggest that for defect-free extrusion over the duration of at least one hour, the fresh concrete should not significantly change consistency. For all of the mixtures that could not be extruded, the stiffness increased more strongly over the measuring period than for the extrudable mixtures. Therefore, for the extrusion of very thin cross sections, as is the case here ( $60 \times 10 \text{ mm}^2$ ), the consistency should be relatively soft in order to allow the deformation of the compound in the mouthpiece from round to the desired thin cross section without errors. In further investigations, the use of superplasticizers or retarders may be useful to positively influence the workability of the concrete. However, it has already been shown in preliminary trials that the use of PCE superplasticizers makes the mixes significantly stickier and thus complicates the extrusion due to the high wall friction. Further research is needed in this area.

It is shown that the differentiation between the individual sphere diameters improves as the sphere diameter increases. The fresh mortar can be described particularly accurately with a sphere diameter of 10 mm. The determined penetration stresses are not similar for the different diameters and increase with decreasing diameters. This is probably due to the different measuring times, as the tests with the sphere diameter of 10 mm were tested after approximately 60 min, those with 15 mm sphere diameter after approximately 40 min and those with 20 mm sphere diameter after approximately 20 min. The fresh concrete stiffens over the measured period.

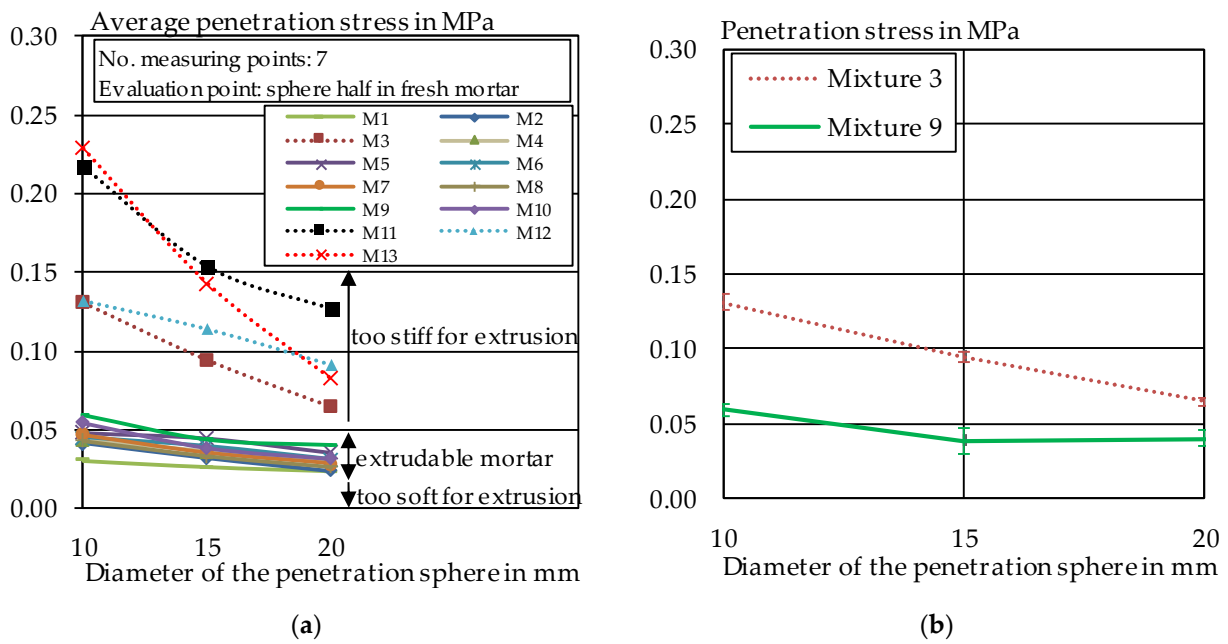


**Figure 14.** (a) Mean penetration stress during penetration tests for the sphere diameters 10 mm, 15 mm and 20 mm for all compounds. Non-extrudable compounds are shown as dotted lines. (b) Results of the penetration tests including scattering of seven individual results for mixture 3 and mixture 9.

The stiffening probably meant that a successful extrusion was not possible. The reason why the mixture rises much faster than the others will be the subject of further research. Based on the results and the laboratory extruder used here, the penetration stress for the extrudable mixtures should be between 0.03 MPa and 0.06 MPa. Figure 14b shows the results of the penetration tests, including the standard deviation for mixture 3 and mixture 9 as an example. Even considering the scatter, the compounds investigated here can be clearly classified as extrudable or non-extrudable, again underlining the suitability of the test to predict the extrudability of mortar mixtures for the LabMorTex. The process thus provides the basis for the production of defect-free, thin, extruded textile concrete elements in the LabMorTex used.

Analogous to the investigations from [38–41] the change in consistency could be recorded with the penetration method. The indentation test is therefore also suitable for the characterisation of even stiffer concretes compared to 3D concrete printing. In 3D concrete printing, indentation tests are mostly used to identify the yield stress and its change over time to determine when the next concrete layer can be printed. Usually a low test speed of, for example, 1  $\mu\text{m}/\text{min}$  in [39] or 0.001  $\mu\text{m}/\text{min}$  or 0.072  $\mu\text{m}/\text{min}$  in [38] is used for this purpose. The results of this work have shown that the penetration test is also suitable for characterising the fresh mortar at a higher speed of 1 mm/min and that an exact determination of the yield point is not necessary to assess whether a mortar is suitable for extrusion with the LabMorTex process.

Thus, the penetration test seems to be the most suitable method to rheologically characterise fresh mortars for the extrusion process with the LabMorTex method, and thus to estimate the extrudability of new mixtures already in the development phase.

Based on the results of the penetration tests, the yield stress for the extrudable mixtures can be estimated approximately to 10–20 kPa according to [39]. In [3,38], 0.05 to 0.1 kPa and in [39] 1–3 kPa are given for the printable concretes in the first 1.5 h. This comparison again shows that the concretes used here are even stiffer than the concretes commonly used in 3D concrete.

The investigations also show that the different approaches of the penetration tests, as they are known from ceramics, can also be used in an adapted form for concrete

extrusion [30,53]. In addition to the rheological characterisation as such, e.g., by determining the yield stress, it could be shown here that, depending on the extruder and the selected mouthpiece, intervals can be fixed to enable fault-free extrusion. In this way, the iterative try and error procedure can be avoided by a targeted fresh concrete characterisation.

The selection of the mixtures investigated here from Table 1 shows only minimal differences in the mixture composition. Compared to mixture 4, only the cement type of mixture 3 was changed from CEM I 42.5 R to CEM III/A 42.5 N, which resulted in the fact that mixture 3 could not be successfully extruded. The results of the mixer data and the capillary rheometer could not clearly show the differences in the mixture composition and the influence on the extrudability. The procedure of the penetration test, as it was applied in this work, is sensitive enough to show the marginal changes in the compound composition and the resulting consistency. Based on the experience at the ibac, this process was able to undercut the durability of the methyl cellulose, since it can lose its effectiveness massively after about one year and mixtures could therefore no longer be extruded. With the method, this effect could be quickly detected and the starting materials replaced accordingly.

With this method, it is possible to react quickly to possible changes due to changing raw materials, process conditions etc. In addition, the penetration method is a simpler measuring method compared to the capillary rheometer, which was used in this work and studied before [8,9,29]. The penetration method presented here also offers the possibility to quickly test the suitability of new material compositions for the plant scale. In addition, the application area of the method can be extended for the characterisation of other materials such as clays or synthetic materials that are also processed in the extrusion process.

## 5. Conclusions

The rheological description of plastic mortars is a challenge for an optimum extrusion process. It is important to determine and control the rheological properties of the fresh mortar to enable a faultless extrusion. Therefore, a variety of test methods have been applied to characterise the rheological properties of fresh mortar before the actual extrusion with the LabMorTex process. The main results achieved are:

- The penetration test allows an accurate, fast and simple classification of the fresh mortar into the classes that are too stiff for extrusion or extrudable for extrusion with the LabMorTex, whereby the fresh mortar can already be characterised before the extrusion process.
- A reduction in the sphere diameter from 20 mm to 10 mm in the penetration test allows a more accurate differentiation of the fresh mortar for the extrusion process, but we are also influenced by the different measurement time.
- The fresh mortar test with a capillary rheometer and the evaluation of the mixer data only allow an initial characterisation of the fresh mortars for the extrusion process. No accurate assessment of extrudability could be obtained.

**Author Contributions:** Conceptualization, methodology, software, validation, formal analysis, investigation, resources, data curation, writing—original draft preparation, M.K.; writing—review and editing, M.K., M.R. and T.M.; visualization, supervision, project administration, M.K.; funding acquisition, M.R. and T.M. All authors have read and agreed to the published version of the manuscript.

**Funding:** This research was funded by Deutsche Forschungsgemeinschaft (DFG, German Research Foundation)—SFB/TRR 280. Projekt-ID: 417002380.

**Data Availability Statement:** Not applicable.

**Acknowledgments:** The work underlying this article was funded by the Deutsche Forschungsgemeinschaft (DFG, German Research Foundation)—SFB/TRR 280. Projekt-ID: 417002380. The authors would like to thank the DFG for supporting the research project.

**Conflicts of Interest:** The authors declare no conflict of interest.

## References

1. Lowke, D.; Dini, E.; Perrot, A.; Weger, D.; Gehlen, C.; Dillenburger, B. Particle-bed 3D printing in concrete construction—Possibilities and challenges. *Cem. Concr. Res.* **2018**, *112*, 50–65. [[CrossRef](#)]
2. Wangler, T.; Lloret, E.; Reiter, L.; Hack, N.; Gramazio, F.; Kohler, M.; Bernhard, M.; Dillenburger, B.; Buchli, J.; Roussel, N.; et al. Digital Concrete: Opportunities and Challenges. *RILEM Tech. Lett.* **2016**, *1*, 67. [[CrossRef](#)]
3. Nicolas, R.; Richard, B.; Nicolas, D.; Irina, I.; Temitope, K.J.; Dirk, L.; Viktor, M.; Romain, M.; Arnaud, P.; Ursula, P.; et al. Assessing the fresh properties of printable cement-based materials: High potential tests for quality control. *Cem. Concr. Res.* **2022**, *158*, 106836. [[CrossRef](#)]
4. Janissen, L.; Raupach, M.; Hartung-Mott, R. Extrusion faserverstärkter Textilbetone. *Bautechnik* **2019**, *96*, 723–730. [[CrossRef](#)]
5. Kalthoff, M.; Raupach, M.; Matschei, T. Investigation into the Integration of Impregnated Glass and Carbon Textiles in a Laboratory Mortar Extruder (LabMorTex). *Materials* **2021**, *14*, 7406. [[CrossRef](#)]
6. Kalthoff, M.; Raupach, M.; Matschei, T. Extrusion and Subsequent Transformation of Textile-Reinforced Mortar Components—Requirements on the Textile, Mortar and Process Parameters with a Laboratory Mortar Extruder (LabMorTex). *Buildings* **2022**, *12*, 726. [[CrossRef](#)]
7. Derby, B.; Händle, F. (Eds.) *Extrusion in Ceramics*; Springer: Berlin/Heidelberg, Germany, 2007; ISBN 978-3-540-27100-0.
8. Alfani, R.; Guerrini, G.L. Rheological test methods for the characterization of extrudable cement-based materials—A review. *Mat. Struct.* **2005**, *38*, 239–247. [[CrossRef](#)]
9. Perrot, A.; Ranguard, D.; Nerella, V.N.; Mechtcherine, V. Extrusion of cement-based materials—An overview. *RILEM Tech. Lett.* **2018**, *3*, 91–97. [[CrossRef](#)]
10. Demont, L.; Ducoulombier, N.; Mesnil, R.; Caron, J.-F. Flow-based pultrusion of continuous fibers for cement-based composite material and additive manufacturing: Rheological and technological requirements. *Compos. Struct.* **2021**, *262*, 113564. [[CrossRef](#)]
11. Kuder, K.G.; Shah, S.P. Rheology of Extruded Cement-Based Materials. *Mater. J.* **2007**, *104*, 283–290. [[CrossRef](#)]
12. Shao, Y.; Qiu, J.; Shah, S.P. Microstructure of extruded cement-bonded fiberboard. *Cem. Concr. Res.* **2001**, *31*, 1153–1161. [[CrossRef](#)]
13. Shao, Y.; Qui, J. The Role of Polymer Additives in Extrusion of Fiber-Cement Composites. *Mater. Spec. Conf. Can. Soc. Civ. Eng.* **2002**, 1–8.
14. Albar, A.; Chougan, M.; Al-Kheetan, M.J.; Swash, M.R.; Ghaffar, S.H. Effective extrusion-based 3D printing system design for cementitious-based materials. *Results Eng.* **2020**, *6*, 100135. [[CrossRef](#)]
15. Buswell, R.A.; Silva, W.R.L.d.; Jones, S.Z.; Dirrenberger, J. 3D printing using concrete extrusion: A roadmap for research. *Cem. Concr. Res.* **2018**, *112*, 37–49. [[CrossRef](#)]
16. Mechtcherine, V.; Bos, F.P.; Perrot, A.; Silva, W.R.L.d.; Nerella, V.N.; Fataei, S.; Wolfs, R.J.M.; Sonebi, M.; Roussel, N. Extrusion-based additive manufacturing with cement-based materials—Production steps, processes, and their underlying physics: A review. *Cem. Concr. Res.* **2020**, *132*, 106037. [[CrossRef](#)]
17. Panda, B.; Unluer, C.; Tan, M.J. Extrusion and rheology characterization of geopolymer nanocomposites used in 3D printing. *Compos. Part B Eng.* **2019**, *176*, 107290. [[CrossRef](#)]
18. Villacis, N.; Gualavisi, M.; Narvaez-Munoz, C.; Carrion, L.; Gualavisi, M. Additive Manufacturing of a Rheological Characterized Cement-Based Composite Material. In Proceedings of the 2017 European Conference on Electrical Engineering and Computer Science (EECS), Bern, Switzerland, 17–19 November 2017; IEEE Computer Society: Los Alamitos, CA, USA, 2017; pp. 326–331, ISBN 978-1-5386-2085-4.
19. Lee, H.; Seo, E.-A.; Kim, W.-W.; Moon, J.-H. Experimental Study on Time-Dependent Changes in Rheological Properties and Flow Rate of 3D Concrete Printing Materials. *Materials* **2021**, *14*, 6278. [[CrossRef](#)]
20. Roussel, N. Rheological requirements for printable concretes. *Cem. Concr. Res.* **2018**, *112*, 76–85. [[CrossRef](#)]
21. Hack, N.; Bahar, M.; Hühne, C.; Lopez, W.; Gantner, S.; Khader, N.; Rothe, T. Development of a Robot-Based Multi-Directional Dynamic Fiber Winding Process for Additive Manufacturing Using Shotcrete 3D Printing. *Fibers* **2021**, *9*, 39. [[CrossRef](#)]
22. Arunothayan, A.R.; Nematollahi, B.; Ranade, R.; Bong, S.H.; Sanjayan, J. Development of 3D-printable ultra-high performance fiber-reinforced concrete for digital construction. *Constr. Build. Mater.* **2020**, *257*, 119546. [[CrossRef](#)]
23. Pham, L.; Tran, P.; Sanjayan, J. Steel fibres reinforced 3D printed concrete: Influence of fibre sizes on mechanical performance. *Constr. Build. Mater.* **2020**, *250*, 118785. [[CrossRef](#)]
24. Suksiripattanapong, C.; Phetprapai, T.; Singsang, W.; Phetchuay, C.; Thumrongvut, J.; Tabyang, W. Utilization of Recycled Plastic Waste in Fiber Reinforced Concrete for Eco-Friendly Footpath and Pavement Applications. *Sustainability* **2022**, *14*, 6839. [[CrossRef](#)]
25. Yoosuk, P.; Suksiripattanapong, C.; Sukontasukkul, P.; Chindaprasirt, P. Properties of polypropylene fiber reinforced cellular lightweight high calcium fly ash geopolymer mortar. *Case Stud. Constr. Mater.* **2021**, *15*, e00730. [[CrossRef](#)]
26. Toutou, Z.; Roussel, N. Multi Scale Experimental Study of Concrete Rheology: From Water Scale to Gravel Scale. *Mater. Struct.* **2007**, *39*, 189–199. [[CrossRef](#)]
27. Laenger, F. Rheology of Ceramic Bodies. In *Extrusion in Ceramics*; Derby, B., Händle, F., Eds.; Springer: Berlin/Heidelberg, Germany, 2007; pp. 141–159, ISBN 978-3-540-27100-0.
28. Göhlert, K.; Uebel, M. Test Methods for Plasticity and Extrusion Behaviour. In *Extrusion in Ceramics*; Derby, B., Händle, F., Eds.; Springer: Berlin/Heidelberg, Germany, 2007; ISBN 978-3-540-27100-0.
29. Andrade, F.A.; Al-Qureshi, H.A.; Hotza, D. Measuring the plasticity of clays: A review. *Appl. Clay Sci.* **2011**, *51*, 1–7. [[CrossRef](#)]

30. Händle, F. Plasticity or the Great Unknown. In *The Art of Ceramic Extrusion*, 1st ed.; Händle, F., Ed.; Springer International Publishing: Imprint Springer: Cham, Switzerland, 2019; pp. 41–48, ISBN 978-3-030-05254-6.
31. de Oliveira Modesto, C.; Bernardin, A.M. Determination of clay plasticity: Indentation method versus Pfefferkorn method. *Appl. Clay Sci.* **2008**, *40*, 15–19. [[CrossRef](#)]
32. Zhou, X. Characterization of rheology of fresh fiber reinforced cementitious composites through ram extrusion. *Mater. Struct.* **2005**, *38*, 17–24. [[CrossRef](#)]
33. Mazzeo, F.A. *Extrusion and Rheology of Fine Particulate Ceramic Pastes*. Ph.D. Thesis, Rutgers State University of New Jersey, New Brunswick, NJ, USA, 2001; Proquest Information and Learning: Ann Arbor, MI, USA, 2001; ISBN 0493094210.
34. Perrot, A.; Rängeard, D.; Mélinge, Y. Prediction of the ram extrusion force of cement-based materials. *Appl. Rheol.* **2014**, *24*, 53320. [[CrossRef](#)]
35. Perrot, A.; Mélinge, Y.; Rängeard, D.; Micaelli, F.; Estellé, P.; Lanos, C. Use of ram extruder as a combined rheo-tribometer to study the behaviour of high yield stress fluids at low strain rate. *Rheol. Acta* **2012**, *51*, 743–754. [[CrossRef](#)]
36. Kuder, K.G.; Shah, S.P. Capillary Rheology of Extruded Cement-Based Materials. In *Measuring, Monitoring and Modeling Concrete Properties*; Konsta-Gdoutos, M.S., Ed.; Springer: Dordrecht, The Netherlands, 2006; pp. 479–484. [[CrossRef](#)]
37. Reiter, L.; Wangler, T.; Anton, A.; Flatt, R.J. Setting on demand for digital concrete—Principles, measurements, chemistry, validation. *Cem. Concr. Res.* **2020**, *132*, 106047. [[CrossRef](#)]
38. Pott, U.; Stephan, D. Penetration test as a fast method to determine yield stress and structural build-up for 3D printing of cementitious materials. *Cem. Concr. Compos.* **2021**, *121*, 104066. [[CrossRef](#)]
39. Lootens, D.; Jousset, P.; Martinie, L.; Roussel, N.; Flatt, R.J. Yield stress during setting of cement pastes from penetration tests. *Cem. Concr. Res.* **2009**, *39*, 401–408. [[CrossRef](#)]
40. Marchment, T. Penetration Reinforcing Method for 3D Concrete Printing. In *Second RILEM International Conference on Concrete and Digital Fabrication: Digital Concrete 2020*, 1st ed.; Bos, F.P., Lucas, S.S., Wolfs, R.J., Salet, T.A., Eds.; Springer International Publishing: Imprint Springer: Cham, Switzerland, 2020; ISBN 9783030499167.
41. Reiter, L.; Wangler, T.; Roussel, N.; Flatt, R.J. Slow penetration for characterizing concrete for digital fabrication. *Cem. Concr. Res.* **2022**, *157*, 106802. [[CrossRef](#)]
42. Alfani, R.; Grizzuti, N.; Guerrini, G.L.; Lezzi, G. The use of the capillary rheometer for the rheological evaluation of extrudable cement-based materials. *Rheol. Acta* **2007**, *46*, 703–709. [[CrossRef](#)]
43. Rubio, M.; Sonebi, M.; Amziane, S. 3D printing of fibre cement-based materials: Fresh and rheological performances. *Acad. J. Civ. Eng.* **2017**, *35*, 480–488. [[CrossRef](#)]
44. Tay, Y.W.D.; Qian, Y.; Tan, M.J. Printability region for 3D concrete printing using slump and slump flow test. *Compos. Part B Eng.* **2019**, *174*, 106968. [[CrossRef](#)]
45. Jayathilakage, R.; Sanjayan, J.; Rajeev, P. Direct shear test for the assessment of rheological parameters of concrete for 3D printing applications. *Mater. Struct.* **2019**, *52*, 12. [[CrossRef](#)]
46. Roussel, N.; Lanos, C.; Toutou, Z. Identification of Bingham fluid flow parameters using a simple squeeze test. *J. Non-Newton. Fluid Mech.* **2006**, *135*, 1–7. [[CrossRef](#)]
47. Dressler, I.; Freund, N.; Lowke, D. The Effect of Accelerator Dosage on Fresh Concrete Properties and on Interlayer Strength in Shotcrete 3D Printing. *Materials* **2020**, *13*, 374. [[CrossRef](#)]
48. Huang, J.; Duan, B.; Cai, P.; Manuka, M.; Hu, H.; Hong, Z.; Cao, R.; Jian, S.; Ma, B. On-demand setting of extrusion-based 3D printing gypsum using a heat-induced accelerator. *Constr. Build. Mater.* **2021**, *304*, 124624. [[CrossRef](#)]
49. Claßen, M.; Ungermann, J.; Sharma, R. Additive Manufacturing of Reinforced Concrete—Development of a 3D Printing Technology for Cementitious Composites with Metallic Reinforcement. *Appl. Sci.* **2020**, *10*, 3791. [[CrossRef](#)]
50. Boscaro, F.; Quadranti, E.; Wangler, T.; Mantellato, S.; Reiter, L.; Flatt, R.J. Eco-Friendly, Set-on-Demand Digital Concrete. *3D Print. Addit. Manuf.* **2022**, *9*, 3–11. [[CrossRef](#)]
51. Kalthoff, M.; Bosbach, S.; Matschei, T.; Raupach, M.; Claßen, M.; Hegger, J. Investigations on material-minimized slabs made of extruded carbon reinforced concrete. In *Proceedings of the Fib International Congress 2022 Oslo*, Oslo, Norway, 12–16 June 2022.
52. Jayathilakage, R.; Rajeev, P.; Sanjayan, J. Extrusion rheometer for 3D concrete printing. *Cem. Concr. Compos.* **2021**, *121*, 104075. [[CrossRef](#)]
53. Händle, F. Measuring the Plasticity of Ceramic Bodies—Part 1. In *Ceramic Forum International (Cfi) 2/2*; Göller Verlag GmbH: Baden-Baden, Germany, 2021.